Journal of Circuits, Systems, and Computers
Vol. 17, No. 4 (2008) 637–658

World Scientific
www.worldscientific.com

HISTORY AND PROGRESS OF THE KERWIN–HUELSMAN–NEWCOMB FILTER GENERATION AND OP AMP REALIZATIONS

AHMED M. SOLIMAN

Electronics and Communication Engineering Department,
Faculty of Engineering, Cairo University, Egypt
asoliman@ieee.org

Revised 20 January 2008

The history of Kerwin–Huelsman–Newcomb (KHN) second-order filter is reviewed. A generation method of the KHN filter from passive RLC filter is presented. Two alternative forms of the KHN circuit using operational amplifier are reviewed. The effect of finite gain-bandwidth of the op amps is considered and expressions of the actual ω_0 and Q are given. Two KHN circuits with inherently stable Q factor are also included. Two new partially compensated inverted KHN circuits are introduced. Active compensation methods to improve the KHN and the inverted KHN circuit performance for high Q designs are summarized. Spice simulation results are given. The progress of the KHN realizations using the current conveyor is also summarized briefly.

Keywords: KHN circuit; active filters; op amps.

1. Introduction

The two most famous multiple output active filter circuits are the Kerwin–Huelsman–Newcomb (KHN) bi-quadratic circuit[1] and the Tow–Thomas bi-quadratic circuit (TT).[2,3] Both circuits are included almost in all textbooks in Active filters,[4–11] and are introduced in most universities to the undergraduate or graduate students. Due to the great importance of these circuits and the progress in their realizations it is desirable to collect such progress in review papers. Recently, the progress in the TT circuit is summarized in a review paper.[12] It is also desirable to provide such a review paper for the KHN circuit, this is the objective of this paper. In the original paper,[1] the theory started by considering a general transfer function of order n, state variable flow graphs with negative gain integrators are used then to develop the insensitive transfer function realization in terms of integrated circuits. The operational amplifier (op amp) is then used to form the integrators and summers needed for the signal flow graph realization. Based on the fact that any polynomial with real coefficients can be factored into first- or second-order degree terms that also have real coefficients, the generalized transfer function can be realized as a cascade of first- and second-order sections. As a consequence,

the work in Ref. 1 concentrates on the realization of the general second-order transfer function using two integrators and two summers. The resulting circuit has four outputs and employs a total of four op amps, two capacitors, and 10 resistors. In most textbooks and for simplicity the summer stage at the output is not included and the three output KHN circuit with highpass, bandpass, lowpass outputs using three op amps is the one that is given in Refs. 4–10. In the next section a generation method to obtain the KHN circuit from a second-order passive RLC circuit is given. The generation method is different from that used in Ref. 12 for the TT circuit in which the resistor and the inductor in the RLC circuit are combined as one impedance unit. In the following generation method the three passive elements in the RLC circuit are taken as separate elements.

2. Generation of KHN Circuit from Passive RLC Circuit

Figure 1(a) represents the passive series RLC filter which is described by the following equations:

$$I = \frac{V_i - V_1}{R_1}, \quad I = \frac{V_1 - V_2}{sL}, \quad V_2 = \frac{1}{sC} I. \tag{1}$$

The above equations can be written in the following form:

$$V_{i1} = \frac{V_i - V_1}{a}, \quad -V_{i1} = \frac{-1}{s\tau_1}(V_1 - V_2), \quad V_2 = \frac{-1}{s\tau_2}(-V_{i1}), \tag{2}$$

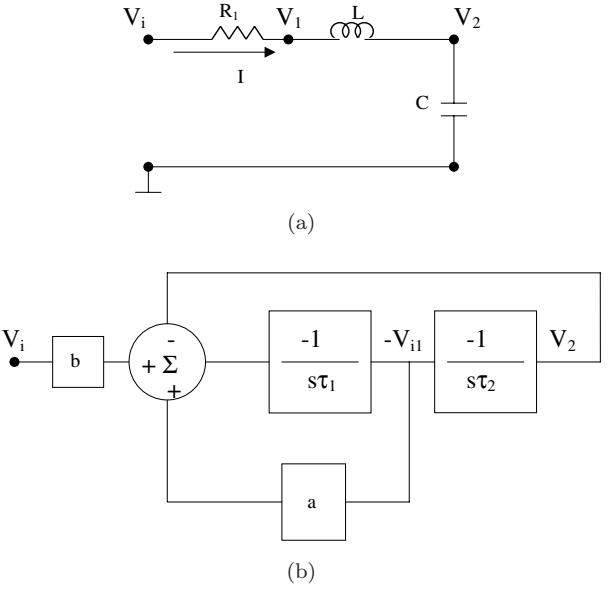

Fig. 1. (a) The passive RLC filter. (b) Block diagram of the passive RLC filter.

where

$$a = \frac{R_1}{R}\,, \quad V_{i1} = IR\,, \quad \tau_1 = \frac{L}{R}\,, \quad \tau_2 = CR\,. \tag{3}$$

The parameter R has the unit of resistor but has no physical existence in the circuit of Fig. 1(a).

Equation (3) can be represented by the block diagram shown in Fig. 1(b), where the parameter b equals to 1 and is added for the purpose of realization of the KHN circuit. It should be noted that although the passive RLC circuit has no feedback paths the block diagram includes two negative feedback loops. The KHN circuit[1] is realizable directly from this block diagram and is shown in Fig. 2(a), with the block diagram parameters given by

$$a = \frac{2R_3}{R_3 + R_4}\,, \quad b = \frac{2R_4}{R_3 + R_4}\,, \quad \tau_1 = C_1R_1\,, \quad \tau_2 = C_2R_2\,. \tag{4}$$

The equivalent block diagram of the circuit of Fig. 2(a) is shown in Fig. 2(b).

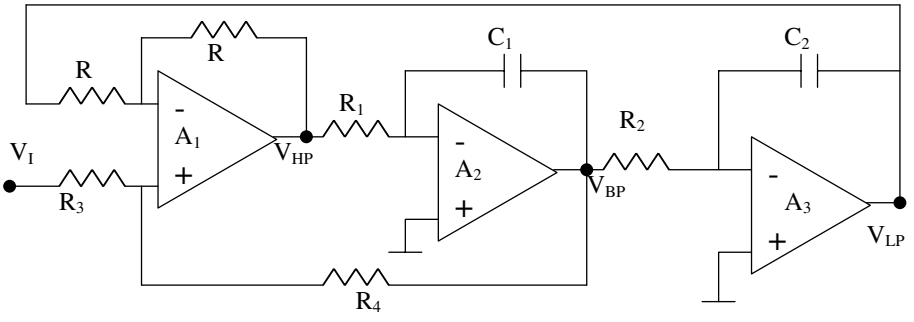

(a)

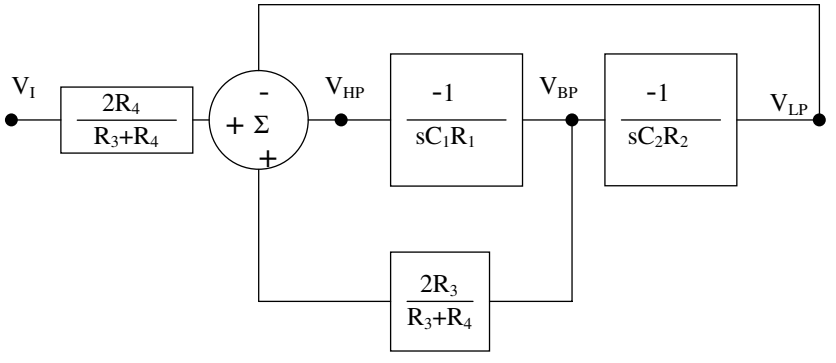

(b)

Fig. 2. (a) The KHN filter.[1] (b) Block diagram of the KHN filter.

The transfer functions of the three outputs at the circuit are given by

$$\begin{aligned}
\frac{V_{\mathrm{HP}}}{V_{\mathrm{I}}} &= \frac{\frac{2R_4}{R_3+R_4}s^2}{s^2 + \frac{2R_3}{R_3+R_4}\cdot\frac{s}{R_1C_1} + \frac{1}{R_1R_2C_1C_2}}\,,\\
\frac{V_{\mathrm{BP}}}{V_{\mathrm{I}}} &= \frac{-\frac{2R_4}{R_3+R_4}\frac{s}{R_1C_1}}{s^2 + \frac{2R_3}{R_3+R_4}\cdot\frac{s}{R_1C_1} + \frac{1}{R_1R_2C_1C_2}}\,,\\
\frac{V_{\mathrm{LP}}}{V_{\mathrm{I}}} &= \frac{\frac{2R_4}{R_3+R_4}\frac{1}{R_1R_2C_1C_2}}{s^2 + \frac{2R_3}{R_3+R_4}\cdot\frac{s}{R_1C_1} + \frac{1}{R_1R_2C_1C_2}}\,.
\end{aligned} \tag{5}$$

The circuit is usually designed by taking equal capacitors $C_1 = C_2 = C$ and the design equations are given by

$$R_1 = R_2 = \frac{1}{\omega_0 C}\,, \quad R_4 = (2Q-1)R_3\,. \tag{6}$$

It is seen that there is independent control on Q by adjusting the value of R_4 without affecting ω_0 of the filter. The magnitude of the gain at ω_0 at any of the three outputs of the filter is given by $2Q-1$.

In this case the parameters a, b in the block diagram of Fig. 2(b) are given by

$$a = \frac{1}{Q}\,, \quad b = 2 - \frac{1}{Q}\,. \tag{7}$$

The filter polarities can be inverted as given by Geffe in the modified KHN circuit published in Ref. 13.

3. Inverted KHN Circuit

In many cases it may be desirable to have a non-inverting bandpass response. The circuit reported in Ref. 13 and shown here in Fig. 3(a) is an inverted version of the KHN circuit. The circuit can also be generated from the passive RLC block diagram of Fig. 1(b) by taking:

$$a = \frac{1}{Q}\,, \quad b = -1\,, \quad \tau_1 = C_1R_1\,, \quad \tau_2 = C_2R_2\,. \tag{8}$$

The transfer functions at the circuit three outputs are given by:

$$\begin{aligned}
\frac{V_{\mathrm{HP}}}{V_{\mathrm{I}}} &= \frac{-s^2}{s^2 + \frac{3R_3}{R_3+R_4}\cdot\frac{s}{R_1C_1} + \frac{1}{R_1R_2C_1C_2}}\,,\\
\frac{V_{\mathrm{BP}}}{V_{\mathrm{I}}} &= \frac{\frac{s}{R_1C_1}}{s^2 + \frac{3R_3}{R_3+R_4}\cdot\frac{s}{R_1C_1} + \frac{1}{R_1R_2C_1C_2}}\,,\\
\frac{V_{\mathrm{LP}}}{V_{\mathrm{I}}} &= \frac{-\frac{1}{R_1R_2C_1C_2}}{s^2 + \frac{3R_3}{R_3+R_4}\cdot\frac{s}{R_1C_1} + \frac{1}{R_1R_2C_1C_2}}\,.
\end{aligned} \tag{9}$$

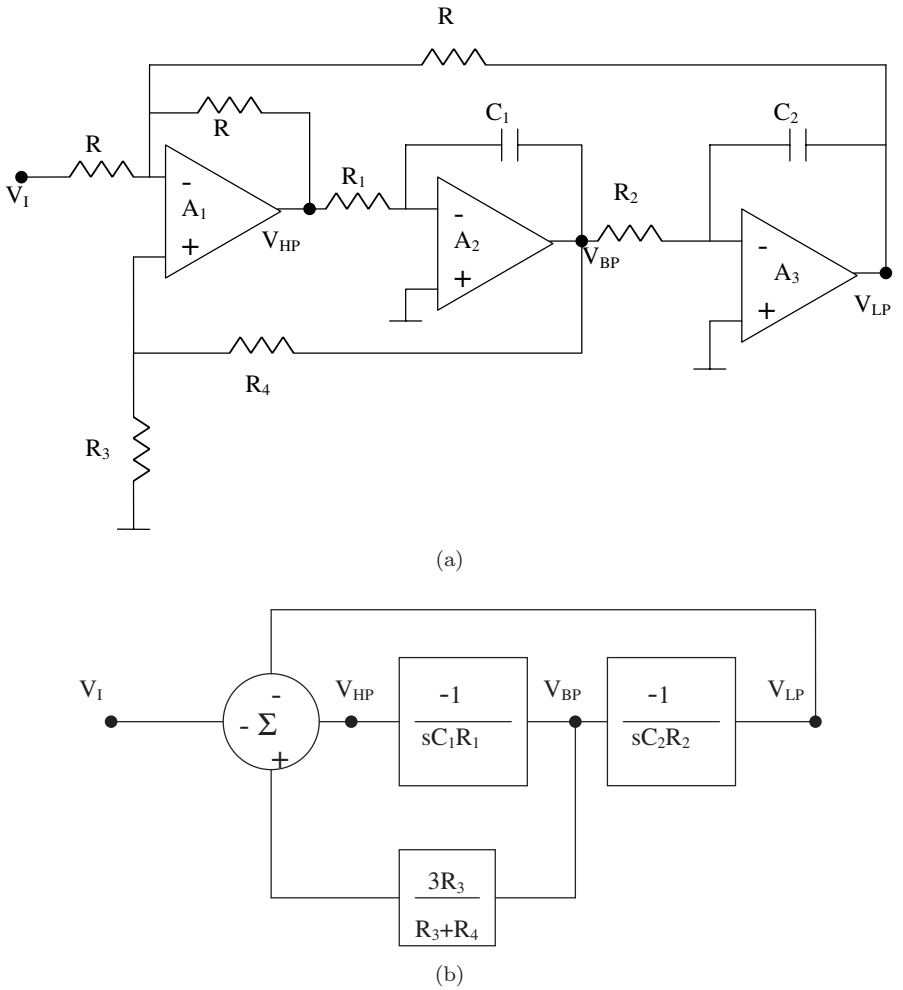

Fig. 3. (a) The inverting input Kerwin–Huelsman–Newcomb filter.[13] (b) Block diagram of the inverting input KHN filter.

Taking equal capacitors $C_1 = C_2 = C$ and the design equations are given by

$$R_1 = R_2 = \frac{1}{\omega_0 C}\,, \quad R_4 = (3Q - 1)R_3\,. \tag{10}$$

It is seen that there is an independent control on Q by adjusting the value of R_4 without affecting ω_0 of the filter. The magnitude of the gain at ω_0 at any of the three outputs of the filter is given by Q.

4. Effect of Finite Gain Bandwidth of the Op Amps

The finite gain bandwidth of the op amp limits the maximum frequency of operation of the KHN circuit and the inverted KHN circuit as well. The frequency limitation

equation of the both circuits take the single pole model of the op amp into consideration is given next. Assume matched op amps are used which are internally compensated to have a single pole open loop response with a unity gain bandwidth ω_t. Thus, the op amp open loop gain is given by

$$A(s) = \frac{A_0\omega_0}{s+\omega_0} \cong \frac{\omega_t}{s}\,. \tag{11}$$

Taking the effect of the finite gain bandwidth into consideration the denominator of the KHN circuit is given by

$$D(s) = \left(s^2 + \frac{\omega_0}{Q}s + \omega_0^2\right) + \frac{s}{\omega_t}\left(4s^2 + \left(\frac{\omega_0}{Q} + 2\omega_0\right)s + \frac{\omega_0^2}{Q}\right). \tag{12}$$

Following Budak–Petrala method[14] the fractional shifts in ω_0 and Q are given approximately by

$$\frac{\Delta\omega_0}{\omega_0} \cong -\frac{\omega_0}{\omega_t}\,, \quad \frac{\Delta Q}{Q} \cong \frac{4\omega_0 Q}{\omega_t}\,. \tag{13}$$

It is seen that the fractional shift in Q is $4Q$ times the fractional shift in ω_0, which sets an upper bound on the maximum frequency of operation for a given op amp and for a specified Q and an allowable limit on the incremental change in Q.

For the inverted KHN, $D(s)$ is given by

$$D(s) = \left(s^2 + \frac{\omega_0}{Q}s + \omega_0^2\right) + \frac{s}{\omega_t}\left(5s^2 + \left(\frac{\omega_0}{Q} + 2\omega_0\right)s + \frac{\omega_0^2}{Q}\right). \tag{14}$$

Following Budak–Petrala method[14] the fractional shifts in ω_0 and Q are given approximately by

$$\frac{\Delta\omega_0}{\omega_0} \cong -\frac{\omega_0}{\omega_t}, \quad \frac{\Delta Q}{Q} \cong \frac{5\omega_0 Q}{\omega_t}\,. \tag{15}$$

It is seen that the fractional shift in Q is 1.25 the shift in Q of the original KHN circuit and is $5Q$ times the fractional shift in ω_0. This sets an upper bound on the maximum frequency of operation for a given op amp and for a specified Q and an allowable limit on the incremental increase in Q.

5. Compensation of the KHN Circuit

As seen in the previous section the KHN circuit and the inverted KHN circuit both suffer from a rather drastic Q-factor-enhancement effect due to the op amps finite gain bandwidth. The Q-factor enhancement is due to the excess phase lag around the loop and hence may be compensated for by the addition of an equal amount of phase lead. The passive compensation methods are not satisfactory solutions as there is no guarantee that the phase cancellation will be valid at different environmental conditions.[15] Before discussing the active compensation methods of the KHN circuit, it is desirable to include here one of the attractive self-compensated three amplifier circuits with stable Q factor.[15]

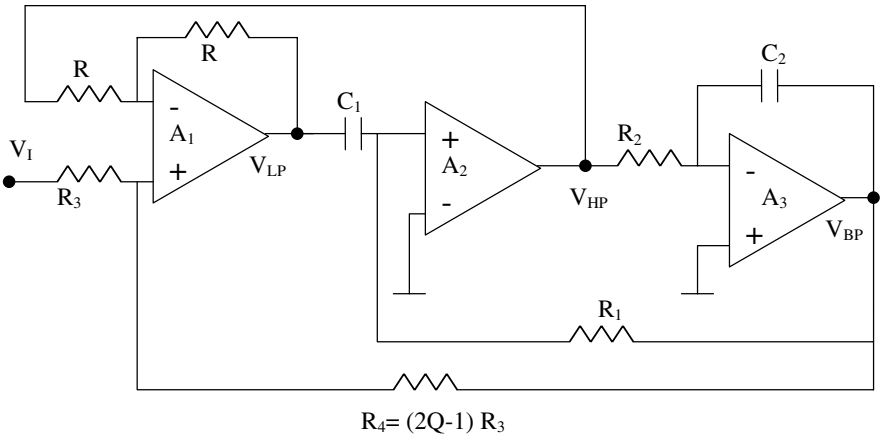

(a)

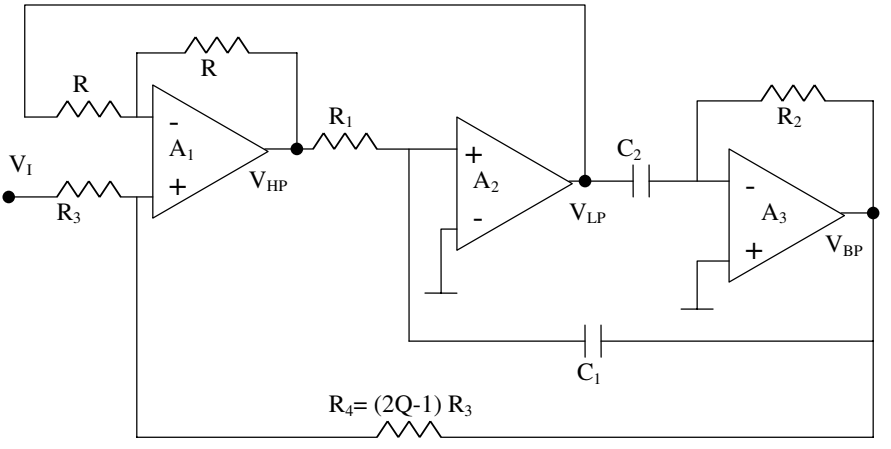

(b)

Fig. 4. (a) Modified KHN circuit 1 with stable Q factor.[15] (b) Modified KHN circuit 2 with stable Q factor.

5.1. *The modified KHN with stable Q factor*

The circuit shown in Fig. 4(a) was introduced in Ref. 15 and is based on the assumption that the three op amps used are matched. The actual Q expression[15] is given by

$$Qa \cong \frac{Q}{1 + Q\left[\frac{2\omega_0}{\omega_{t1}} - \frac{\omega_0}{\omega_{t2}} - \frac{\omega_0}{\omega_{t3}}\right]}. \tag{16}$$

For matched op amps it is seen that the circuit is almost free from Q-factor error.

The circuit shown in Fig. 4(b) is related to that shown in Fig. 4(a) by RC:CR transformation[6] of the two integrator elements. It can also be generated from the

KHN circuit of Fig. 2(a) by representing the op amps by the nullators and norators and exchanging the outputs of the two integrator stages. It is possible to generate many more circuits based on the interchange of the two ports of the three nullors,[16] however the circuit of Fig. 4(a) is the most attractive one.

5.2. *Active compensation of the KHN circuit*

Phase correction in the KHN circuit can be achieved if the phase lead integrator reported in Ref. 17 is used in place of one of the two integrators as shown in Fig. 5(a). The phase lead of the integrator that is used in Fig. 5(a) is given by

$$\phi \cong K\frac{\omega_0}{\omega_{t4}}\left(\frac{a}{K+1}-1\right). \tag{17}$$

Assuming matched op amps are used and taking $K = 1$; and to provide the necessary phase lead of $3\omega_0/\omega_t$, it is seen that a should be taken equal to 8.

Another active compensated KHN circuit is shown in Fig. 5(b) which is based on adding the phase corrector consisting of op amp number 4 and two resistors.[18] The phase lead of the summer stage is adjusted to $2\omega_0/\omega_t$ to cancel the two integrators phase lag.

It should be noted that the circuits of Fig. 5 are better than the self-compensated circuits of Fig. 4 as they can be used with mismatched op amps.

6. Compensation of the Inverted KHN Circuit

Figure 6(a) represents a partially compensated inverted KHN circuit obtained by interchanging the two integrator outputs. Five more new circuits can be obtained from Fig. 3(a) based on the interchange of the two ports of the three nullors.[16] The circuit shown in Fig. 6(b) is related to that shown in Fig. 6(a) by RC:CR transformation[6] of the two integrator elements. It can be proved that for the circuit in Fig. 6(a), the fractional shift in Q is one fifth of its value for the circuit in Fig. 3(a). It can also be proved that for the circuit in Fig. 6(b) the fractional shift in Q is the negative of one fifth of its value for the circuit in Fig. 3(a).

Phase correction in the inverted KHN circuit can be achieved if the phase lead integrator reported in Ref. 17 is used in place of one of the two integrators as shown in Fig. 7(a).

Assuming matched op amps are used and taking $K = 1$; and to provide the necessary phase lead of $4\omega_0/\omega_t$, and using Eq. (17) it is seen that a should be taken equal to 10.

Another active compensated inverted KHN circuit is shown in Fig. 6(b) which is based on adding the phase corrector consisting of op amp number 4 and two resistors.[18] The phase lead of the summer stage is adjusted to $2\omega_0/\omega_t$ in order to cancel the two integrators phase lag.

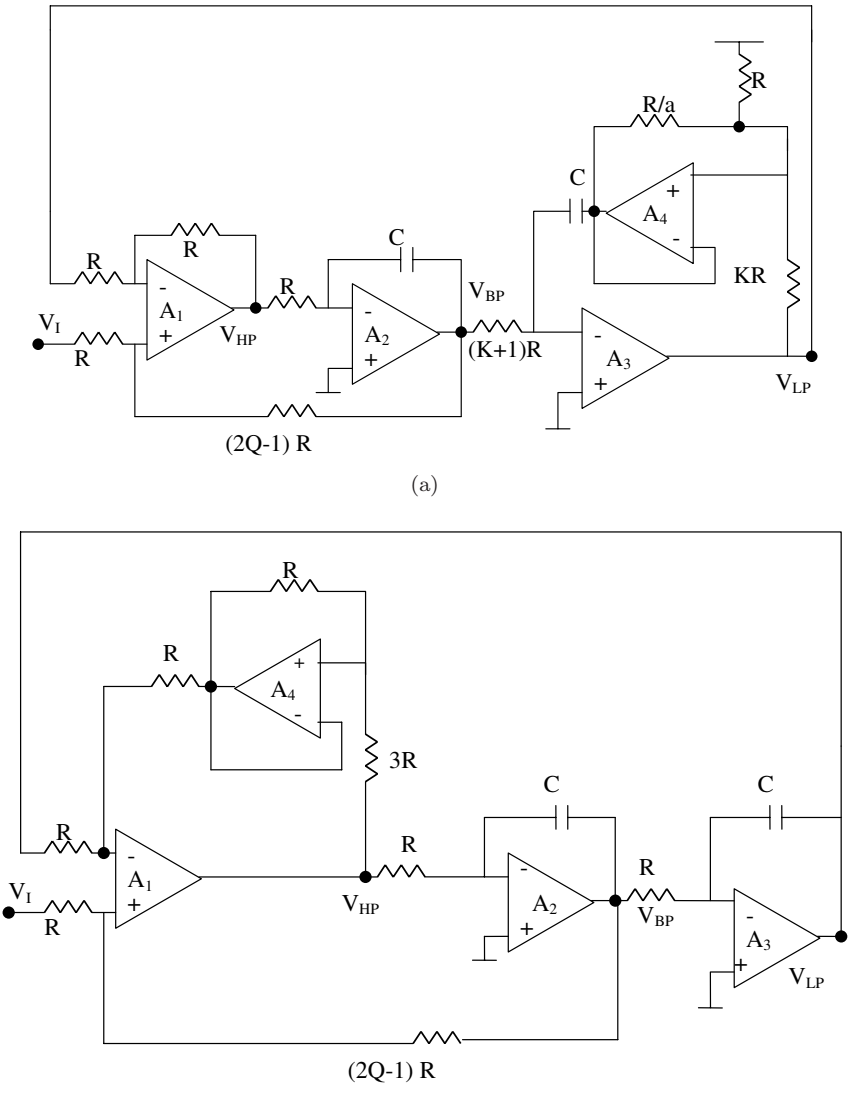

Fig. 5. (a) Active compensated KHN circuit using phase lead inverting integrator.[17] (b) Active compensated KHN circuit using phase corrector.[18]

7. Spice Simulations

In this section, spice simulations are carried out using the op amp μA 741 from Analog Devices with $f_t = 1\,\text{MHz}$ and using supply voltages of $\pm 15\,\text{V}$. The KHN circuit of Fig. 2(a) is designed for $Q = 5$ and $f_0 = 10\,\text{kHz}$ taking $C_1 = C_2 = 500\,\text{pF}$, $R_1 = R_2 = 31.9\,\text{k}\Omega$, $R = 10\,\text{k}\Omega$, $R_3 = 10\,\text{k}\Omega$, $R_4 = 90\,\text{k}\Omega$ and using sinusoidal input voltage source of 1 V magnitude.

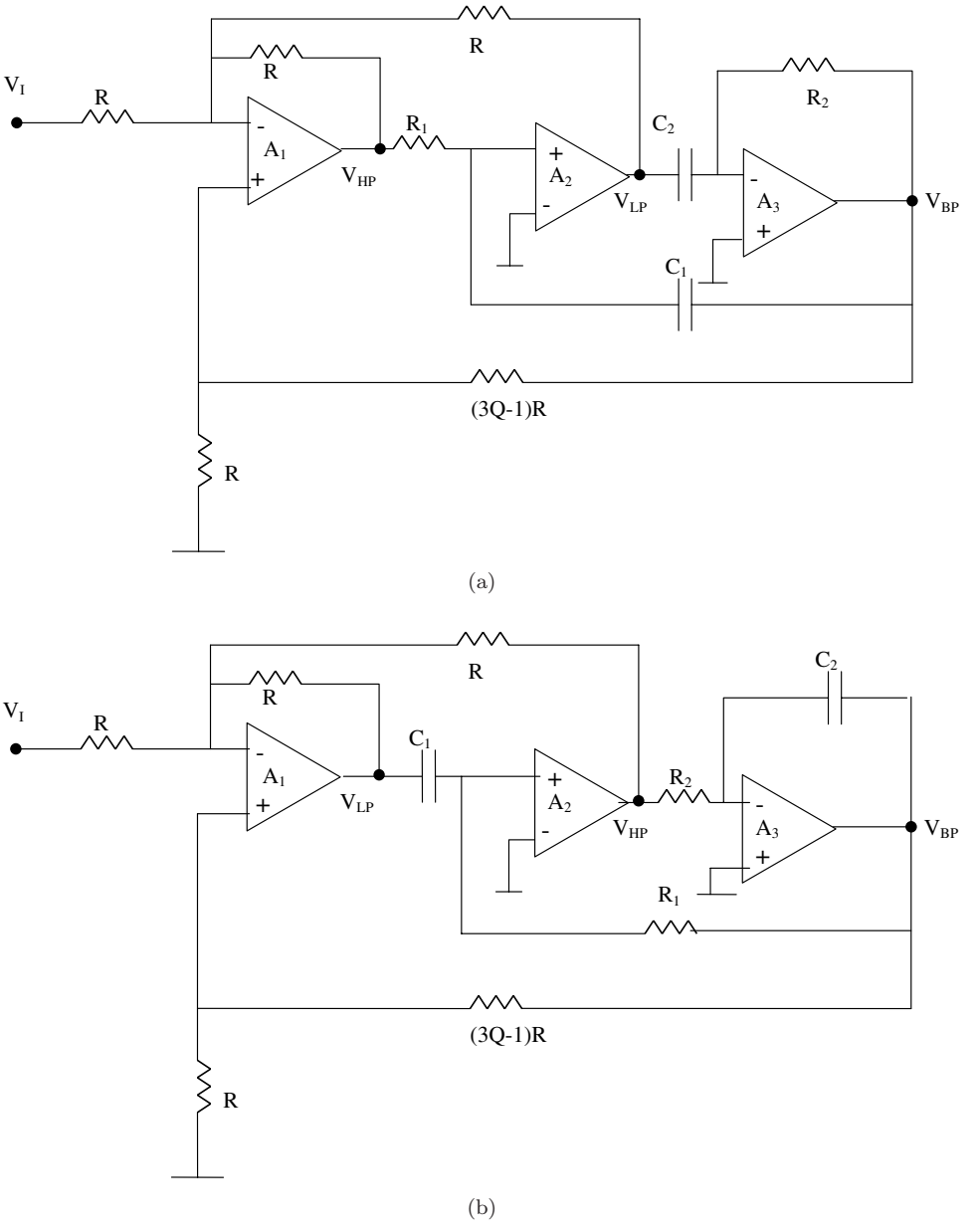

Fig. 6. (a) The first partially compensated inverted KHN circuit. (b) The second partially compensated inverted KHN circuit.

Figure 8(a) represents the spice simulation results of the magnitude and phase of the KHN circuit together with the ideal response. Since the gain at the center frequency equals to $2Q-1$, and from the linear scale simulated magnitude it is seen that the center frequency gain $= 11$, hence it is seen that Q has increased from its

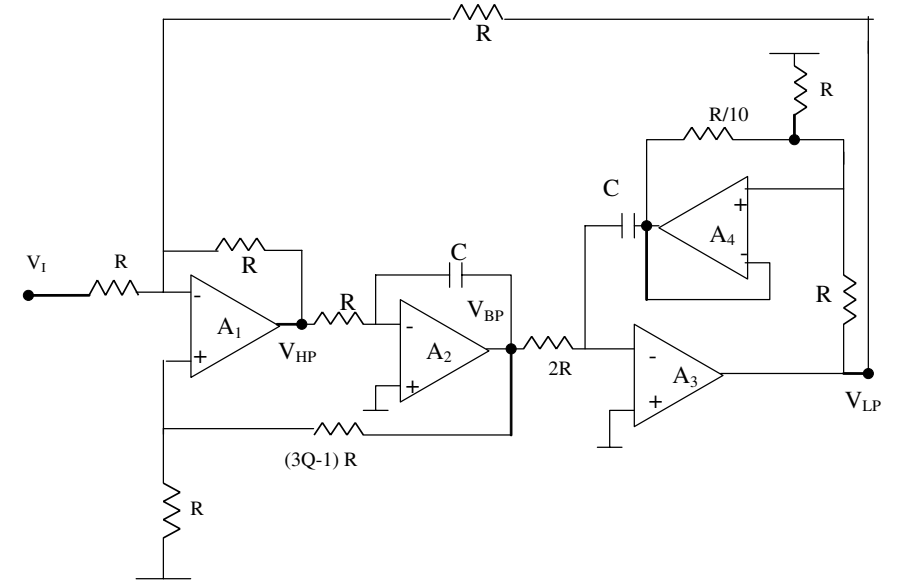

(a)

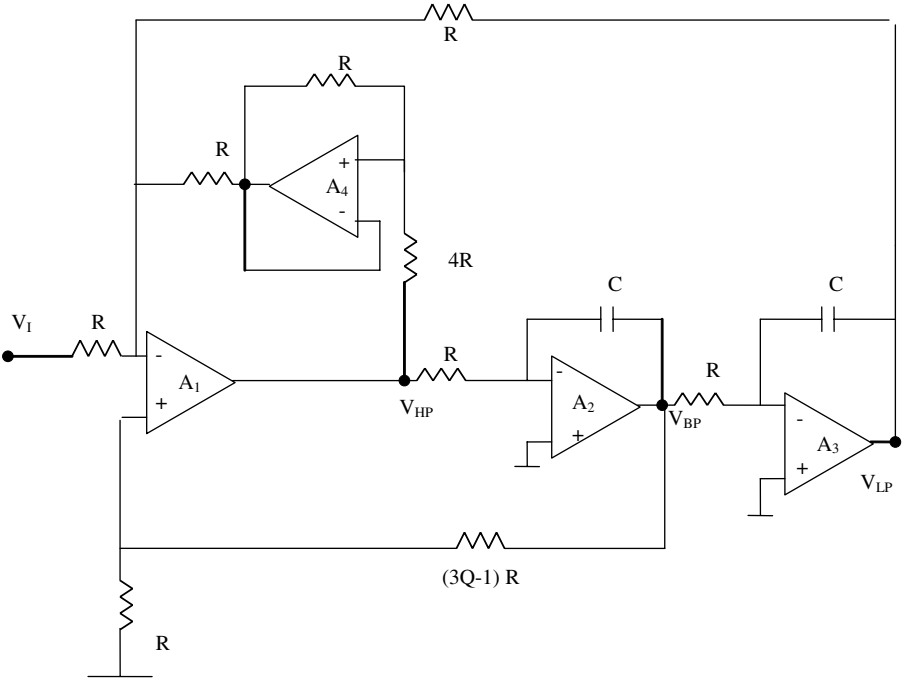

(b)

Fig. 7. (a) Active compensated inverted KHN circuit using phase lead inverting integrator. (b) Active compensated inverted KHN circuit using phase corrector.

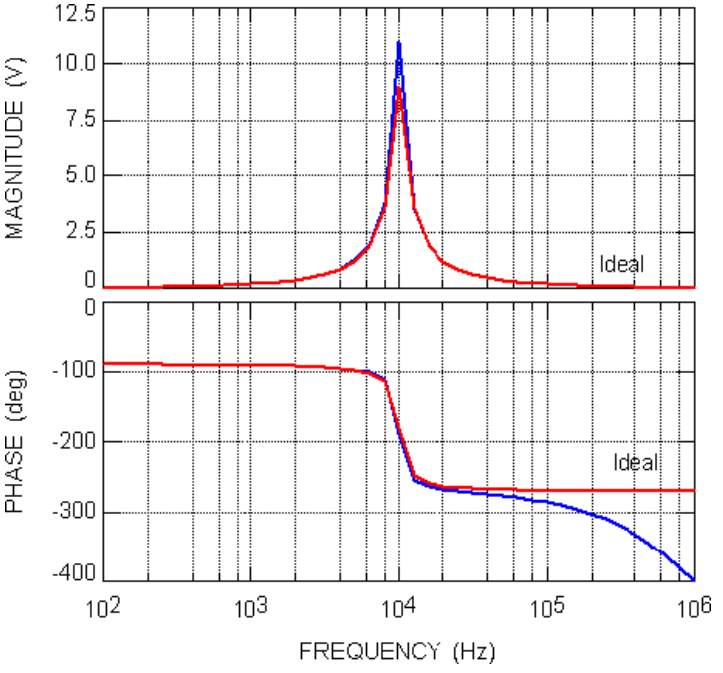

(a)

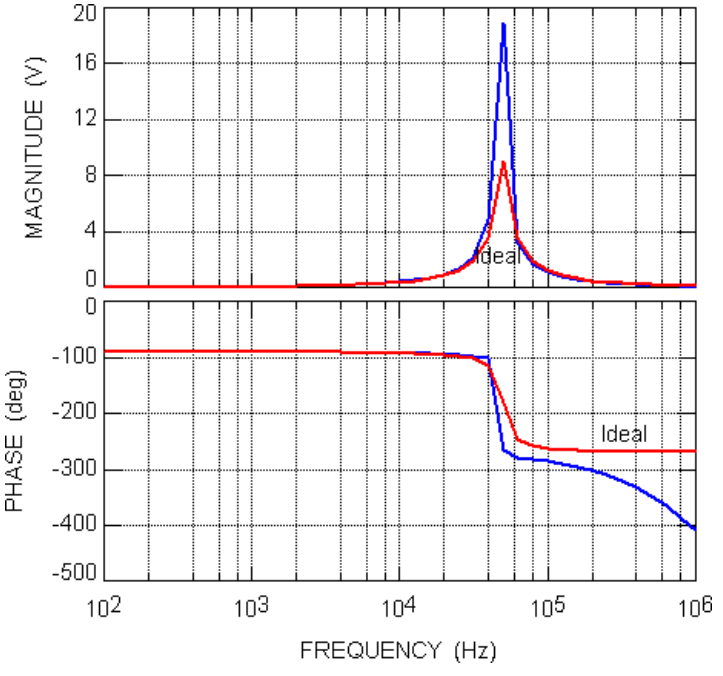

(b)

Fig. 8. Simulation results of the magnitude and phase characteristics of KHN circuit of Fig. 2(a) at (a) 10 kHz and at (b) 50 kHz.

theoretical value of 5 to $Q_a = 6$. From the simulation results $\Delta Q/Q = 0.2$ which is the same as the theoretical expected value obtained from Eq. (13).

Figure 8(b) represents the spice simulation results of the magnitude and phase of the KHN circuit designed with the same Q value as the previous circuit and with $f_0 = 50\,\text{kHz}$ taking $C_1 = C_2 = 100\,\text{pF}$ and all resistors the same as before. It is seen that the center frequency gain = 19, hence $Q_a = 10$ which is double the ideal value of 5, and $\Delta Q/Q = 1$ which is the same as the theoretical expected value obtained from Eq. (13).

The inverted KHN circuit of Fig. 3(a) is designed for $Q = 5$ and $f_0 = 10\,\text{kHz}$ taking $C_1 = C_2 = 500\,\text{pF}$, $R_1 = R_2 = 31.9\,\text{k}\Omega$, $R = 10\,\text{k}\Omega$, $R_3 = 10\,\text{k}\Omega$, $R_4 = 140\,\text{k}\Omega$ and using sinusoidal input voltage source of 1 V magnitude.

Figure 9(a) represents the spice simulation results of the magnitude and phase of the KHN circuit together with the ideal response. Since the gain at the center frequency equals to Q, and from the linear scale simulated magnitude it is seen that the center frequency gain = 6.4, hence it is seen that Q has increased from its theoretical value of 5 to $Q_a = 6.4$. From the simulation results $\Delta Q/Q = 0.28$ which is very close to the theoretical value of 0.25 obtained from Eq. (15).

Figure 9(b) represents the spice simulation results of the magnitude and phase of the inverted KHN circuit designed with the same Q value as the previous circuit and with $f_0 = 50\,\text{kHz}$ taking $C_1 = C_2 = 100\,\text{pF}$ and all resistors the same as before. It is seen that the center frequency gain = 10, hence $\Delta Q/Q = 1$ which is smaller than the theoretical expected value of $\Delta Q/Q = 1.25$ obtained from Eq. (15).

Figure 10(a) represents the spice simulation results of the magnitude and phase of the modified KHN circuit of Fig. 4(a) designed for $Q = 5$ and $f_0 = 10\,\text{kHz}$ and taking same circuit values as for the KHN circuit of Fig. 2(a). From the simulations it is seen that the simulated Q is 5 as its theoretical value.

Figure 10(b) represents the spice simulation results of the magnitude and phase of the modified KHN circuit of Fig. 4(b) designed for $Q = 5$ and $f_0 = 10\,\text{kHz}$ and taking same circuit values as for the KHN circuit of Fig. 2(a). From the simulations it is seen that the simulated Q is 5 as its theoretical value.

Figures 11(a) and 11(b) represent the simulation results of the two active compensated KHN circuits of Figs. 5(a) and 5(b) for $Q = 5$ and $f_0 = 50\,\text{kHz}$.

Figures 12(a) and 12(b) represent the simulation results of the two new inverted KHN circuits of Figs. 6(a) and 6(b) for $Q = 5$ and $f_0 = 50\,\text{kHz}$. From the simulations of Fig. 12(a) it is seen that Q is slightly higher than its ideal value, and from Fig. 12(b) it is slightly lower than its ideal value of 5 as expected.

Figures 13(a) and 13(b) represent the simulation results of the two active compensated inverted KHN circuits of Figs. 7(a) and 7(b) for $Q = 5$ and $f_0 = 50\,\text{kHz}$.

8. KHN Circuit Using Current Conveyors

Due to the frequency limitation of the KHN circuit using op amps it is desirable to increase the frequency range of operation using the current conveyors (CCII). The

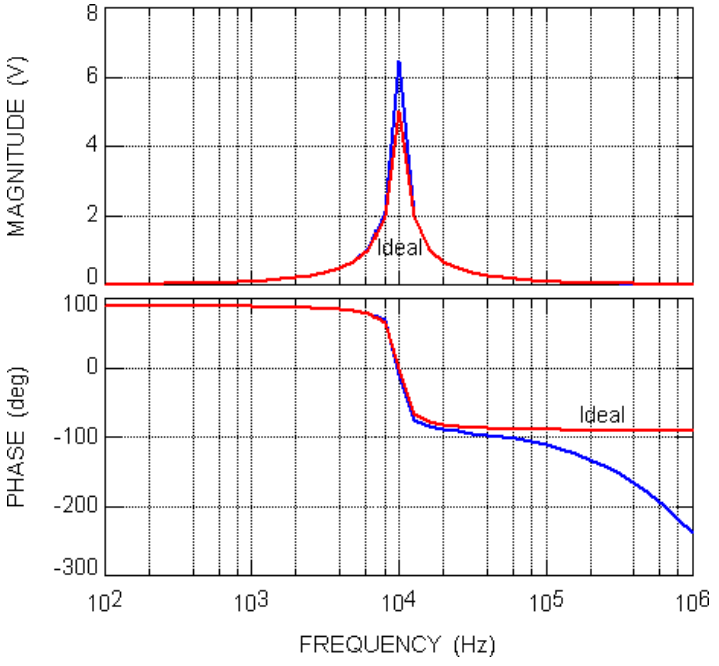

(a)

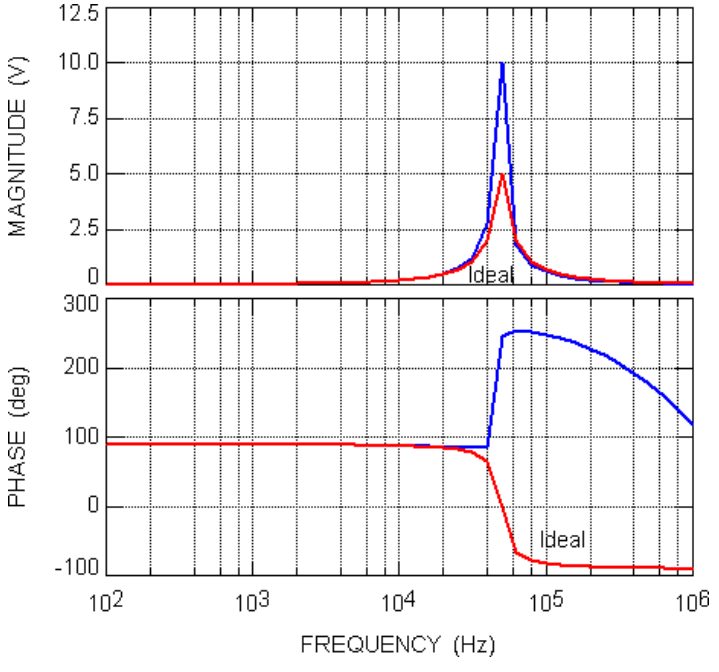

(b)

Fig. 9. Simulation results of the magnitude and phase characteristics of the circuit of Fig. 3(a) at (a) 10 kHz and at (b) 50 kHz.

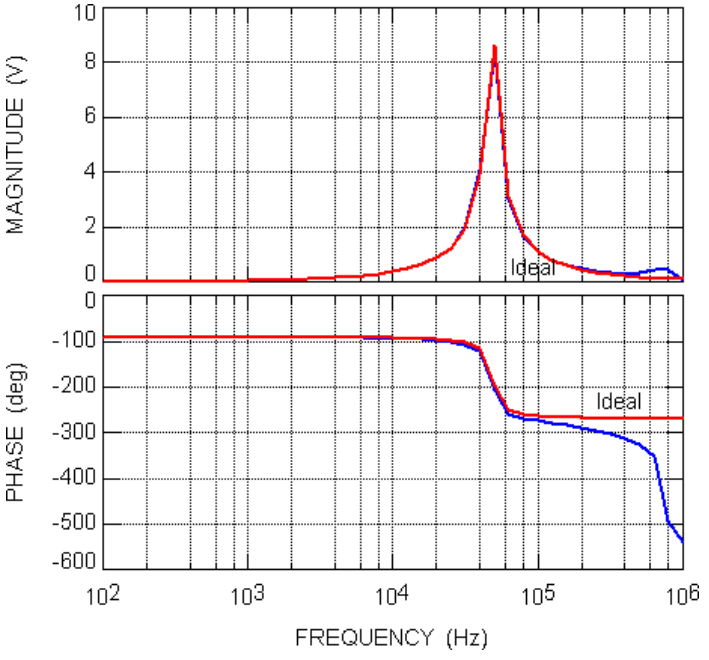

(a)

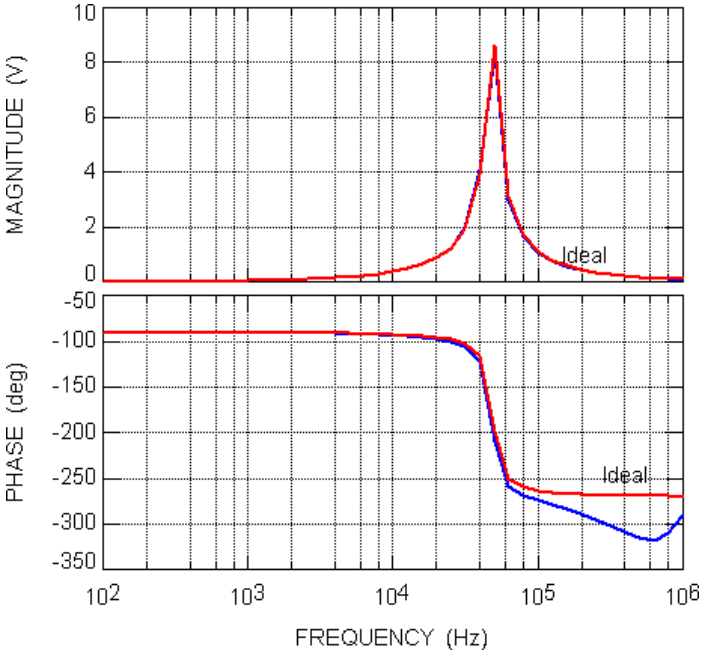

(b)

Fig. 10. (a) Simulation results of the magnitude and phase characteristics of the circuit of Fig. 4(a) at 50 kHz. (b) Simulation results of the magnitude and phase characteristics of the circuit of Fig. 4(b) at 50 kHz.

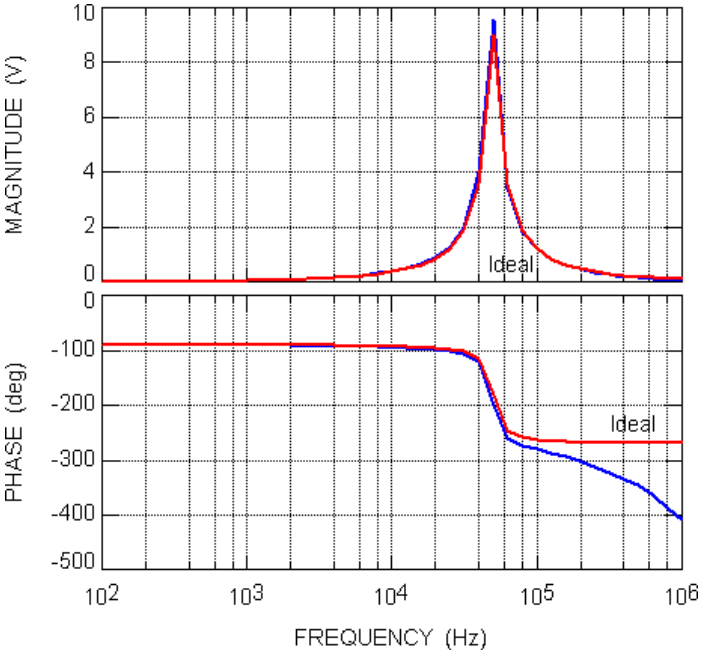

(a)

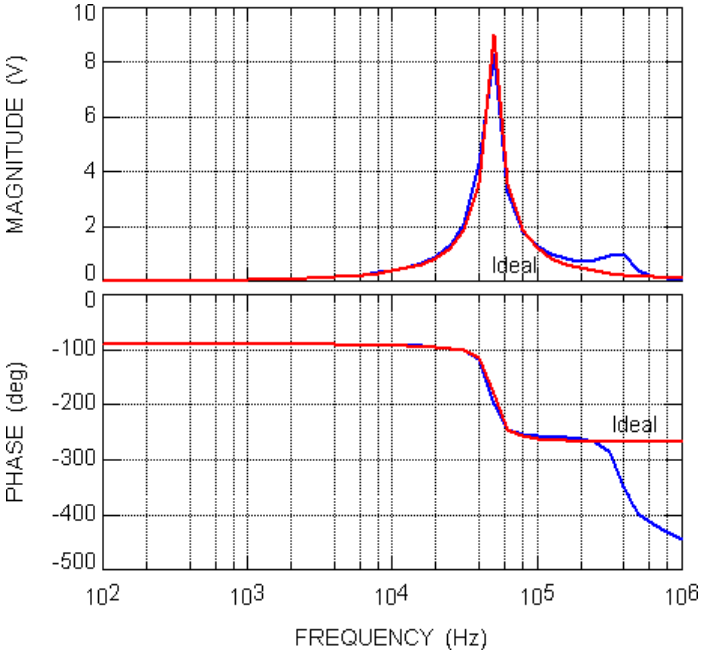

(b)

Fig. 11. (a) Simulation results of the magnitude and phase characteristics of the circuit of Fig. 5(a) at 50 kHz. (b) Simulation results of the magnitude and phase characteristics of the circuit of Fig. 5(b) at 50 kHz.

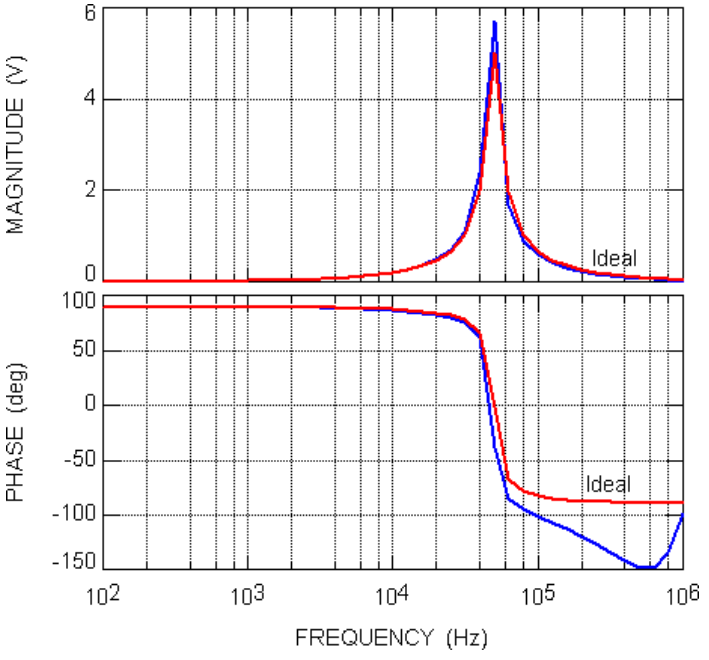

(a)

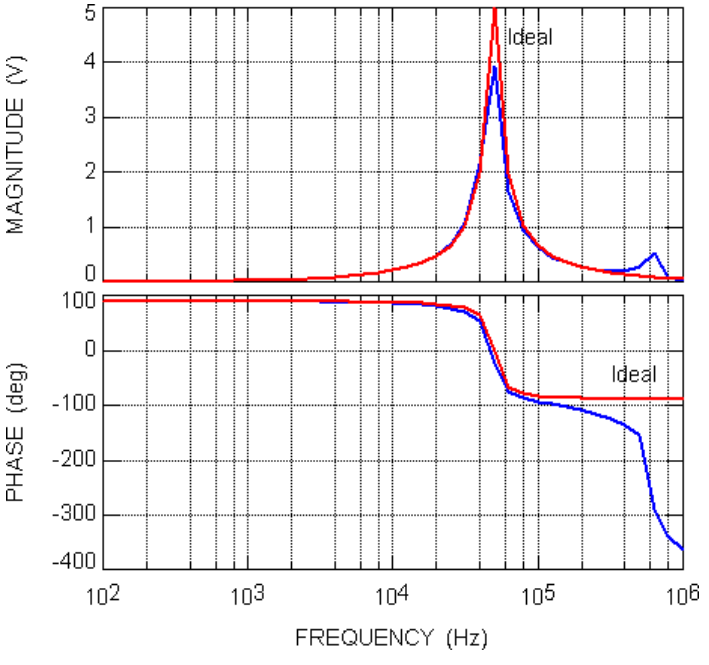

(b)

Fig. 12. (a) Simulation results of the magnitude and phase characteristics of the circuit of Fig. 6(a) at 50 kHz. (b) Simulation results of the magnitude and phase characteristics of the circuit of Fig. 6(b) at 50 kHz.

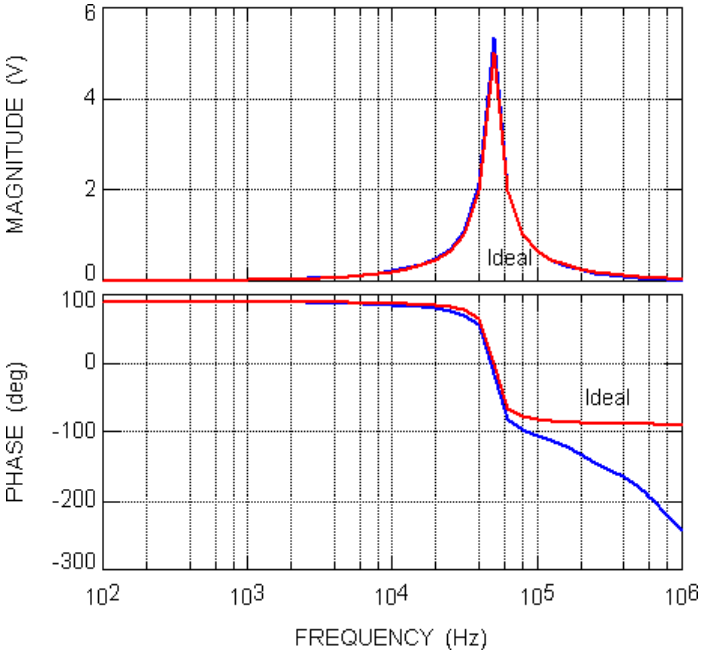

(a)

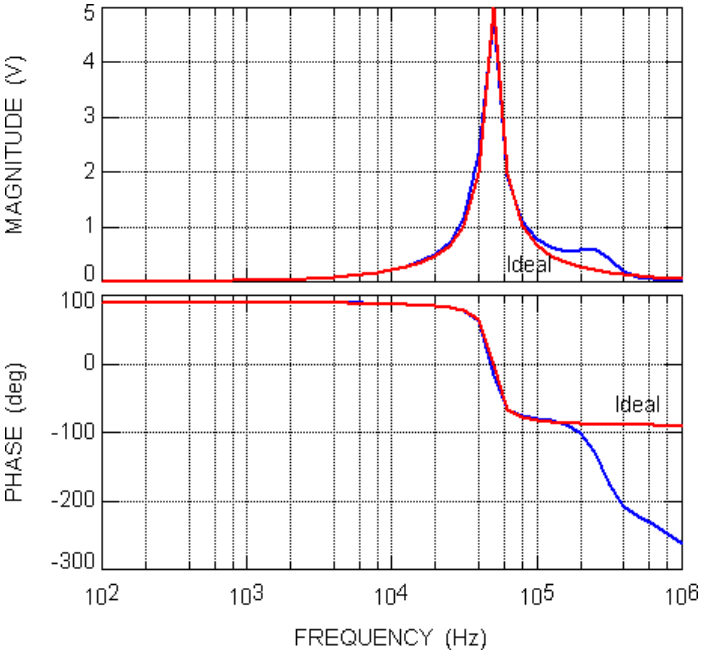

(b)

Fig. 13. (a) Simulation results of the magnitude and phase characteristics of the circuit of Fig. 7(a) at 50 kHz. (b) Simulation results of the magnitude and phase characteristics of the circuit of Fig. 7(b) at 50 kHz.

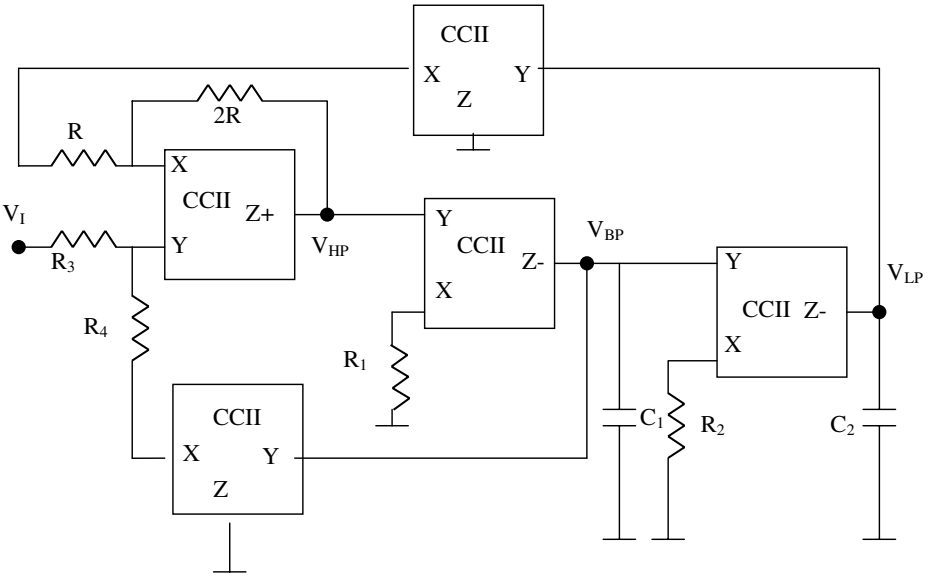

(a)

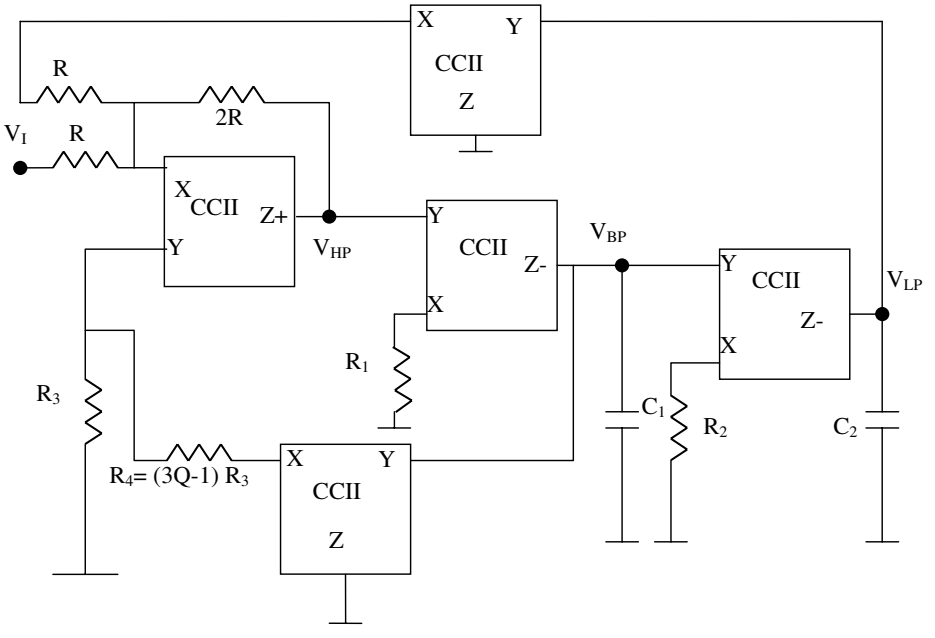

(b)

Fig. 14. (a) The grounded capacitor KHN circuit using current conveyors.[19] (b) The grounded capacitor inverted KHN using current conveyors. (c) The grounded resistor grounded capacitor KHN circuit using five CCII+.[20]

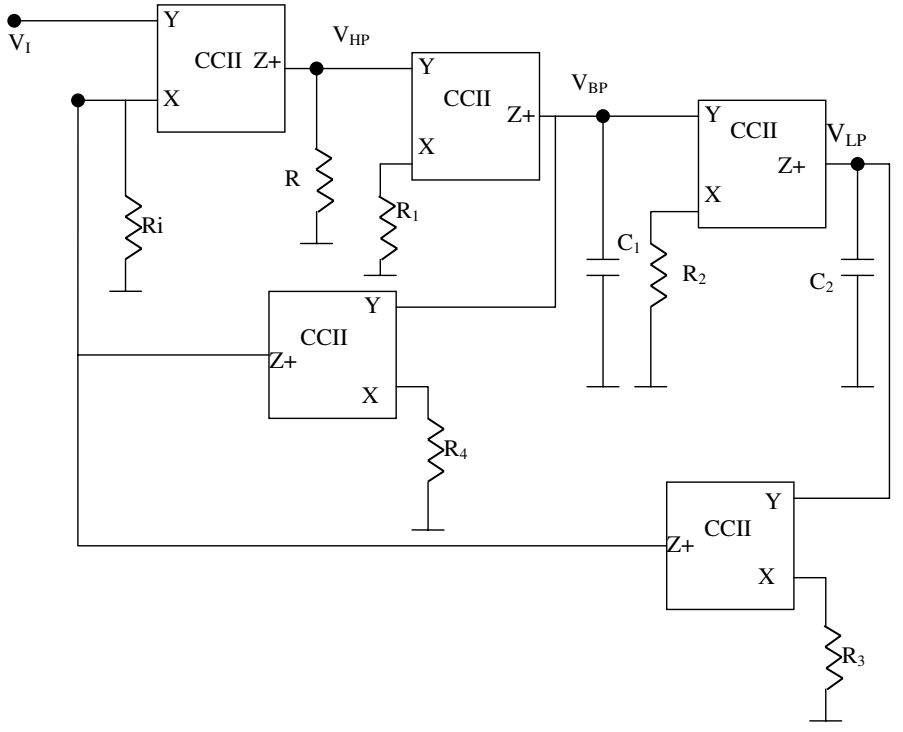

(c)

Fig. 14. (*Continued*)

first KHN circuit using CCII was introduced in Ref. 19 and is shown in Fig. 14(a). This circuit has identical equations to the KHN circuit of Fig. 2(a) and it has the advantage of using two grounded capacitors.

Figure 14(b) represents a new grounded capacitor realization of the inverted KHN circuit using current conveyors. It has the same equations as the inverted KHN circuit of Fig. 3(a) and is also represented by the block diagram of Fig. 3(b).

A further progress in the KHN circuit was achieved by the introduction of the grounded resister grounded capacitor circuit shown in Fig. 14(c).[20] This circuit can realize all the eight sign polarities combinations of the three output voltages by proper choice of the CCII polarities as explained in Ref. 20. The circuit can employ five CCII+ as shown to realize three non-inverting filter responses. It has the additional advantages of very high input impedance; the gain can be adjusted by varying R_i without affecting ω_0 or Q of the filter. Also the Q of the filter can be adjusted by R_4 independent of ω_0 and the gain.

Further progress in universal filters was achieved by the introduction of the MOS-C current mode circuit in Ref. 21 which employs three balanced output modified differential current conveyors (MDCC), six MOS transistors and two grounded capacitors.

9. Conclusions

The KHN circuit and the inverted KHN circuit are generated from the passive RLC filter circuit. The effect of the finite gain bandwidth on both the KHN and the inverted KHN is summarized. The self-compensated KHN circuit is reviewed as well as the modified KHN circuit obtained by interchanging the op amp outputs of the two integrators. Simulation results are included to demonstrate the practicality of both circuits as well the active compensated KHN circuits. Two new partially compensated inverted KHN circuits are reported together with their simulation results. The active compensation methods are also applied to the inverted KHN circuit to provide stable Q universal filters.

The progress of the KHN realizations using the current conveyor is also summarized very briefly. Further progress in the KHN realization using the operational transresistance amplifier (OTRA) has also been introduced in the literature[22,23] and is not included here to limit the paper length.

References

1. W. Kerwin, L. Huelsman and R. Newcomb, State variable synthesis for insensitive integrated circuit transfer functions, *IEEE J. Solid State Circuit* **2** (1967) 87–92.
2. J. Tow, A step by step active filter design, *IEEE Spectrum* **6** (1969) 64–68.
3. L. Thomas, The Biquad: Part I — Some practical design considerations, *IEEE Trans. Circuit Theory* **18** (1971) 350–357.
4. T. Deliyannis, Y. Sun and J. K. Fidler, *Continuous Time Active Filter Design* (CRC Press, 1999), pp. 146–147.
5. M. S. Ghausi and K. R. Laker, *Modern Filter Design, Active RC and Switched Capacitor* (Prentice Hall, Engelwood Cliffs, NJ, 1981), pp. 226–227.
6. M. E. Van Valkenburg, *Analog Filter Design* (Holt Rinehart and Winston, 1982), pp. 136–137.
7. A. Budak, *Passive and Active Network Analysis and Synthesis* (Houghton Mifflin, 1974), pp. 356–365.
8. A. S. Sedra and K. C. Smith, *Microelectronic Circuits* (Oxford University Press, 1998), pp. 927–929.
9. H.-Y.-F. Lam, *Analog and Digital Filters* (Prentice Hall, 1979), pp. 401–417.
10. L. P. Huelsman and P. E. Allen, *Introduction to Theory and Design of Active Filters* (McGraw Hill, 1980), pp. 258–269.
11. S. K. Mitra, *Active Inductor-Less Filters* (IEEE Press, 1971).
12. A. M. Soliman, History and progress of the Tow–Thomas circuit: Part I, generation and op amp realizations, *J. Circuits Syst. Comput.* **17** (2008) 33–54.
13. P. R. Geffe, RC amplifier resonators for active filters, *IEEE Trans. Circuit Theory* **15** (1968) 415–419.
14. A. Budak and D. Petrala, Frequency limitations of active filters using operational amplifiers, *IEEE Trans. Circuit Theory* **CT-19** (1972) 322–328.
15. L. Brown and A. S. Sedra, New multifunction biquadratic filter circuit with inherently stable Q factor, *Electron. Lett.* **13** (1977) 719–721.
16. S. M. Chang and G. M. Wierzba, Circuit level decomposition of networks with nullors for symbolic analysis, *IEEE Trans. Circuits Syst. I* **41** (1994) 699–711.

17. A. M. Soliman, Novel phase lead inverting integrator and its application in two integrator loop filters, *Electron. Lett.* **16** (1980) 475–476.
18. A. M. Soliman and M. Ismail, A universal variable phase 3-Port VCVS and its applications in two integrator loop filters, in *Proc. IEEE Int. Symp. Circuits and Systems*, Houston, Texas (1980), pp. 83–86.
19. A. M. Soliman, Kerwin–Huelsman–Newcomb circuit using current conveyors, *Electron. Lett.* **30** (1994) 2019–2020.
20. A. M. Soliman, Current conveyor steer universal filter, *IEEE Circuits Dev. Mag.* (1995) 45–46.
21. H. O. Elwan and A. M. Soliman, CMOS differential current conveyors and applications for analog VLSI, *Analog Integr. Circuits Signal Process.* **11** (1996) 35–45.
22. K. N. Salama and A. M. Soliman, CMOS operational transresistance amplifier for analog signal processing, *Microelectron. J.* **30** (1999) 235–245.
23. K. N. Salama and A. M. Soliman, Voltage mode Kerwin–Huelsman–Newcomb circuit using CDBAs, *Frequeny* **54** (2000) 90–93.